



RESEARCH ARTICLE | JUNE 27 2024

Recurrent chaotic clustering and slow chaos in adaptive networks

Special Collection: [Advances in Adaptive Dynamical Networks](#)Matheus Rolim Sales   ; Serhiy Yanchuk  ; Jürgen Kurths 

Chaos 34, 063144 (2024)

<https://doi.org/10.1063/5.0205458>

Chaos

Special Topic:
Anomalous Diffusion and Fluctuations
in Complex Systems and Networks

[Submit Today](#)

Recurrent chaotic clustering and slow chaos in adaptive networks

Cite as: Chaos 34, 063144 (2024); doi: 10.1063/5.0205458

Submitted: 26 February 2024 · Accepted: 5 June 2024 ·

Published Online: 27 June 2024



View Online



Export Citation



CrossMark

Matheus Rolim Sales,^{1,2,3,a)} Serhiy Yanchuk,^{3,4} and Jürgen Kurths^{3,5}

AFFILIATIONS

¹Department of Physics, São Paulo State University, Rio Claro 13506-900, SP, Brazil

²Graduate Program in Sciences, State University of Ponta Grossa, Ponta Grossa 84030-900, PR, Brazil

³Potsdam Institute for Climate Impact Research, Member of the Leibniz Association, P.O. Box 6012 03, Potsdam D-14412, Germany

⁴School of Mathematical Sciences, University College Cork, Western Road, Cork T12 XF62, Ireland

⁵Institute of Physics, Humboldt University Berlin, Berlin 10099, Germany

Note: This paper is part of the Focus Issue on Advances in Adaptive Dynamical Networks.

a) Author to whom correspondence should be addressed: rolim.sales@unesp.br

ABSTRACT

Adaptive dynamical networks are network systems in which the structure co-evolves and interacts with the dynamical state of the nodes. We study an adaptive dynamical network in which the structure changes on a slower time scale relative to the fast dynamics of the nodes. We identify a phenomenon we refer to as recurrent adaptive chaotic clustering (RACC), in which chaos is observed on a slow time scale, while the fast time scale exhibits regular dynamics. Such slow chaos is further characterized by long (relative to the fast time scale) regimes of frequency clusters or frequency-synchronized dynamics, interrupted by fast jumps between these regimes. We also determine parameter values where the time intervals between jumps are chaotic and show that such a state is robust to changes in parameters and initial conditions.

Published under an exclusive license by AIP Publishing. <https://doi.org/10.1063/5.0205458>

Many complex dynamical systems have a network structure that evolves (adapts) over time. Such systems are typical in neural learning systems but also occur in a variety of other applications. A typical scenario is when the network structure changes much slower than the dynamics of each individual node. In such cases, many exciting multiscale phenomena occur that are impossible in systems with a static network structure. In this paper, we present the phenomenon of recurrent adaptive chaotic clustering (RACC) in which the network structure changes slowly and chaotically, while the node dynamics is fast and regular. In addition, the fast dynamics recurrently changes from complete frequency synchrony to frequency clusters of different types.

I. INTRODUCTION

Adaptive dynamical networks (ADN) appear in various applications ranging from neuroscience^{1–3} to social^{4–7} or transportation⁸ networks. While dynamical networks with static connectivity can describe synchronization phenomena and pattern formation in

networks with static structure,^{9,10} ADNs allow a dynamic change of the network structure and an interaction between this structural dynamics and the dynamics of the network nodes.^{11,12} ADNs are fundamental models for describing the learning of neuronal systems due to neuronal plasticity.^{2,13}

ADNs exhibit exciting new dynamical phenomena such as frequency clusters,^{14–19} recurrent synchronization,²⁰ self-organized noise resistance,³ self-organized criticality,²¹ heterogeneous nucleation,²² and others. For a more detailed overview, we refer to the recent review¹¹ and references therein. Despite being a versatile class of models suitable for many applications, ADNs are challenging for a theoretical or numerical study due to their complexity, which is usually reflected in their high dimensionality, multistability, or the presence of multiple time scales.^{23,24}

This paper reports on the phenomenon of recurrent adaptive chaotic clustering (RACC) in ADNs. More specifically, we describe the emergence of a robust dynamical regime in which the system exhibits “quasi-stationary” frequency clusters of various types. The frequency clusters exist for a relatively long time, followed by a rapid transition to another cluster or to a frequency-synchronized

regime. The main difference with the previously reported recurrent switching in ADNs²⁰ is that in our case the switching between these quasi-stationary regimes is chaotic, and, thus, the length of each clustering episode cannot be predicted for a longer time. Looking at the observed phenomenon from the point of view of the theory of multiscale systems, the reported effect represents *slow chaos*, where the chaotic dynamics is manifested on the slow timescale of the coupling weights, but the fast dynamics is regular. To understand this phenomenon in detail, we consider a minimal model of ADN with three oscillators and six slowly changing couplings.

The structure of the paper is as follows. In Sec. II, we introduce the concept of adaptive dynamical networks and describe the model under study in this paper. In Sec. III, we present numerical evidence of RACC for a minimal model of three phase oscillators for specific parameter values, and in Sec. IV, we show that such a behavior is robust to changes in parameters. In Sec. V, we compute the Lyapunov exponents and show that the dynamics of the system can be chaotic and the largest Lyapunov exponent is positive for a large range of parameters. In Sec. VI, we present the new type of slow chaotic dynamics and demonstrate that chaotic clustering exhibits different partially synchronized states. Section VII contains our final remarks.

II. ADAPTIVE DYNAMICAL NETWORK MODEL

A dynamical network^{25–28} is defined as a set of N nodes, or vertices, and L links, or edges. The topology of the connections is given by the weighted connectivity matrix $A = \{\kappa_{ij}\}$, $i, j = 1, 2, \dots, N$, with nonzero real elements if the node j is connected to the node i and 0 otherwise. The state of the network is given by $\mathbf{x} = (\mathbf{x}_1, \mathbf{x}_2, \dots, \mathbf{x}_N)$, where $\mathbf{x}_i \in \mathbb{R}^d$ is the d -dimensional state variable of each individual node, and its dynamics can be written as

$$\dot{\mathbf{x}}_i = f_i(\mathbf{x}_i, t) + \sum_{j=1}^N \kappa_{ij} \Gamma_{ij}(\mathbf{x}_i, \mathbf{x}_j, t), \quad (1)$$

where f_i defines the local dynamics of each node and $\Gamma_{ij}(\mathbf{x}_i, \mathbf{x}_j, t)$ is the coupling function. By allowing the coupling weights to dynamically adapt depending on the state and the history of each node, the network structure becomes part of the temporal evolution and is not static anymore. We call such a system an adaptive dynamical network (ADN)^{11,12,29,30} and define it as

$$\dot{\mathbf{x}}_i = f_i(\mathbf{x}_i, t) + \sum_{j=1}^N \kappa_{ij} \Gamma_{ij}(\mathbf{x}_i, \mathbf{x}_j, t), \quad (2)$$

$$\dot{\kappa}_{ij} = g_{ij}(\mathbf{x}_i, \mathbf{x}_j, t), \quad (3)$$

with $g(\mathbf{x}_i, \mathbf{x}_j, t)$ being the adaptation function depending explicitly on the state of the nodes i and j . This allows the network structure to rearrange according to the states of the nodes, which in turn are affected by this structure.

The interest in ADN of the form (2)–(3) has grown significantly over the last years,^{11,30} and several forms of adaptation rules have been proposed in order to describe different dynamical systems and phenomena.^{31–34} One basic type of adaptation rule that has gained a

lot of attention recently is the following:^{14,15,20,35–37}

$$\dot{\mathbf{x}}_i = f_i(\mathbf{x}_i) + \sum_{j=1}^N \kappa_{ij} \Gamma_{ij}(\mathbf{x}_i, \mathbf{x}_j), \quad (4)$$

$$\dot{\kappa}_{ij} = -\varepsilon [\kappa_{ij} + a_{ij} h_{ij}(\mathbf{x}_i - \mathbf{x}_j)], \quad (5)$$

where it is assumed that the adaptation function $h_{ij}(\mathbf{x}_i - \mathbf{x}_j)$ depends only on the difference of the corresponding state vectors, analogous to the spike-timing-dependent plasticity (STDP).^{1,13,38} The base connectivity structure is given by the matrix elements $a_{ij} \in \mathbb{R}$ and the parameter $\varepsilon > 0$ is a timescale separation parameter.

In particular, we are interested in slow adaptation, which means $\varepsilon \ll 1$. Then, the dynamics of the nodes, Eq. (4), is much faster than the dynamics of the network, and tools from the geometric singular perturbation theory can be used to study such systems.^{24,39–42} Indeed, the slow-fast dynamics is one of the essential ingredients for the emergence of recurrent synchronization²⁰ or excitability⁴³ in adaptive networks. With the slow change of the coupling weights κ_{ij} , the dynamics in the fast layer (\mathbf{x}) can exhibit different synchrony patterns recurrently for different weights κ .

Here, we are interested in the dynamics and synchronization of coupled nonlinear oscillator systems. Models of phase oscillators, such as the paradigmatic Kuramoto⁴⁴ and Kuramoto-Sakaguchi⁴⁵ models, have been of major importance in the development of the theory of synchronization, and it is widely known that we can reduce a network of coupled nonlinear oscillators to a network of phase oscillators given weak interactions.^{10,46,47} Therefore, following Eqs. (4)–(5), we consider a network of N adaptively coupled phase oscillators given by

$$\dot{\phi}_i = \omega_i - \frac{1}{N} \sum_{j=1}^N \kappa_{ij} \sin(\phi_i - \phi_j + \delta), \quad (6)$$

$$\dot{\kappa}_{ij} = -\varepsilon [\kappa_{ij} + a_{ij} \sin(\phi_i - \phi_j + \beta_{ij})], \quad (7)$$

where $\phi_i \in [0, 2\pi)$. We consider the same coupling and adaptation functions for each pair of phase oscillators, and ω_i is the natural frequency of the i th oscillator. The parameter δ can be considered as a phase lag of the interaction,⁴⁵ and different β_{ij} control the non-homogeneity of the adaptation function.^{15,22,35}

In the following Sec. III, we investigate the collective dynamics of the network (6)–(7) with three phase oscillators, which is a minimal model exhibiting RACC. For most numerical simulations, the initial conditions are chosen randomly, with the phases, ϕ_i , distributed uniformly in the interval $[0, 2\pi)$ and the coupling weights, κ_{ij} , in $[-1, 1]$, unless explicitly stated otherwise. All numerical integration in this paper is performed using the 4th order Runge-Kutta method implemented in Fortran.

III. CHAOTIC RECURRENT CLUSTERING: NUMERICAL EVIDENCE

To measure the collective dynamics of the network, we use an observable that provides an average of the individual nodes'

dynamics, namely, the Kuramoto order parameter, $R(t)$, given by

$$R(t) = \frac{1}{N} \left| \sum_{j=1}^N e^{i\phi_j(t)} \right|. \quad (8)$$

$R(t)$ measures the global phase synchronization of the network. If, at a certain instant of time t , the phases are the same, $R(t) = 1$, whereas, if the phases are spread incoherently over the interval $[0, 2\pi)$, $R(t) = 0$. Furthermore, by following the temporal evolution of $R(t)$, we can detect different synchronization states, such as frequency synchronization, which corresponds to a slowly changing $R(t)$ during some time interval, and the loss of phase relation, which corresponds to a rapidly oscillatory behavior of $R(t)$, in which we observe partial or no frequency synchronization.²⁰

The phenomenon of recurrent synchronization corresponds to alternating time intervals of high activity, i.e., fast changes of the collective observable, and time intervals of low activity. It has been reported by Thiele *et al.*²⁰ for two populations of Hodgkin–Huxley neurons⁴⁸ with asymmetric STDP, for a reduced model of only two interacting Hodgkin–Huxley neurons with asymmetric STDP, and also for two adaptively coupled phase oscillators with asymmetric adaptation rules, defined by Eqs. (6) and (7). Here, we study three adaptively coupled phase oscillators, and our choice of parameters is inspired by the work of Thiele *et al.*²⁰ We choose the connectivity matrix elements a_{ij} in such a way that there is no connection between oscillators 2 and 3, i.e., $a_{23} = a_{32} = 0$. We fix all parameters to the values shown in Table I, and a_{13} , which corresponds to the amplitude of the influence of oscillator 3 on oscillator 1, is considered as active parameter. To quantify frequency synchronization,

TABLE I. Parameters used in the simulations.

Parameter	Value
$\Omega_1 = \omega_1 - \omega_2$	0.1
$\Omega_2 = \omega_1 - \omega_3$	0.12
ε	2.0×10^{-4}
δ	$\pi/4$
a_{12}	0.375
a_{21}	1.5
a_{23}	0.0
a_{31}	1.2
a_{32}	0.0
β_{12}	$4\pi/3$
β_{13}	$1 + \pi$
β_{21}	$\pi/2$
β_{31}	$-3\pi/2 + 0.1$

we measure the mean phase velocity of each oscillator as

$$\langle \dot{\phi}_i \rangle = \frac{1}{T} \int_{T_0}^{T_0+T} \dot{\phi}_i(t) dt \quad (9)$$

in windows of size $T = 300$ and say that oscillators i and j are frequency synchronized if $|\langle \dot{\phi}_i \rangle - \langle \dot{\phi}_j \rangle| < 0.01$. If all oscillators are synchronized to each other, we have complete synchronization and one single cluster, labeled as $C_{\{i,j,k\}}$. When only two oscillators are synchronized, we have partial synchronization and two clusters, one composed of two synchronized oscillators and one composed of a single asynchronous one. We label this state as $C_{\{i,j\},k}$. For the case of complete asynchrony, we have three clusters and label this state as $C_{i,j,k}$.

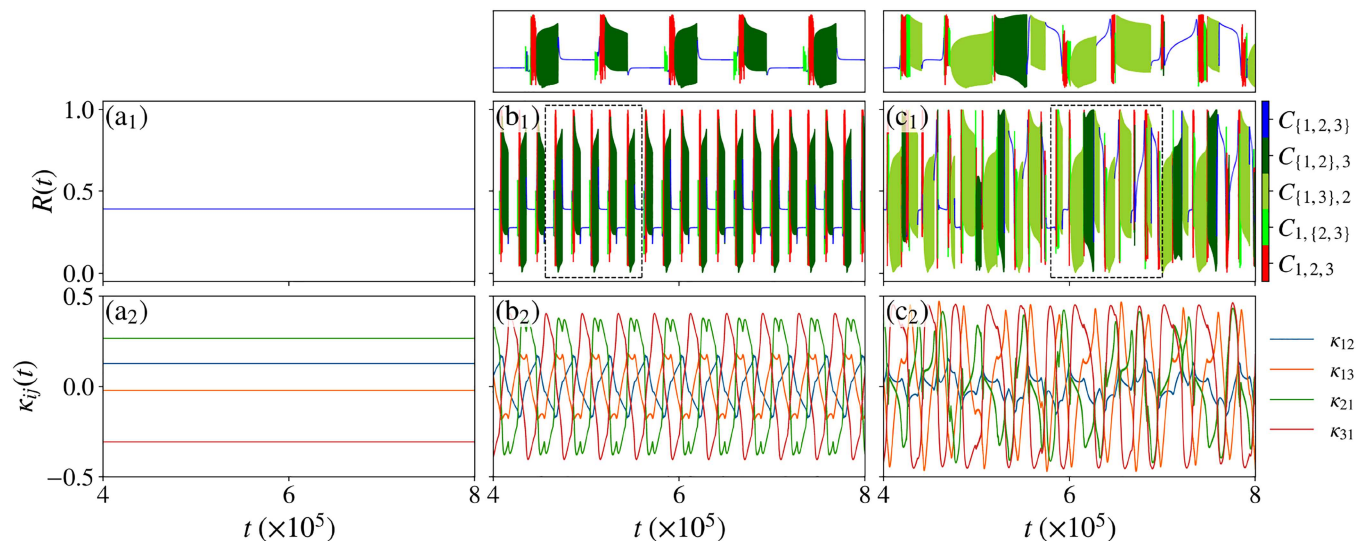


FIG. 1. The order parameter, $R(t)$ [Eq. (8)], and the coupling weights, $\kappa_{ij}(t)$, as a function of time for the parameters in Table I with (a) $a_{13} = 0.1$, (b) $a_{13} = 0.6$, and (c) $a_{13} = 1.1$. The top row shows magnifications in the order parameter for the corresponding regions in the dashed boxes.

Depending on the value of a_{13} , we can obtain different solutions for this model, such as the trivial fixed point solution for the coupling weights, κ_{ij} [Fig. 1(a)]. This corresponds to a constant value of the $R(t)$ and complete frequency synchronization, and we do not observe recurrent synchronization. As we increase the value of a_{13} , recurrent synchronization emerges [Fig. 1(b)]. We clearly observe several transitions between slow changing to a fast oscillating order parameter, with slow periodic oscillations in the coupling weights during the whole depicted interval. The color scale in the first row indicates all possible synchronization states, with blue, green (all three), and red representing complete, partial, and no synchronization, respectively. In Fig. 1(b), there is a seemingly periodic transition among these synchronization states. For larger values of a_{13} , the transition turns out to be rather irregular [Fig. 1(c)], and we observe no periodicity in either the order parameter or the coupling weights.

Interestingly, for some periods of time, oscillators 2 and 3 are synchronized even though there is no direct link between them [light green in Figs. 1(b) and 1(c)]. Such a phenomenon is known as relay (or remote) synchronization,^{49,50} i.e., synchronization between two not directly connected oscillators in a network.

IV. NUMERICAL BIFURCATION ANALYSIS OF THE RECURRENT ADAPTIVE CHAOTIC CLUSTERING

In order to study the influence of the parameters and the robustness of this newly observed phenomenon, RACC, we compute

the value of one of the coupling weights, κ_{12} , when each synchronization (clustering) state begins and the time spent in each one of them as a function of the parameter a_{13} (Fig. 2). The choice of the observable κ_{12} is not important here, only that it is one of the slow coupling variables κ_{ij} , since the fast phase variables fluctuate on a faster timescale.

We use random initial conditions for $a_{13} = 0$ and for each new parameter value, the initial condition corresponds to the last state of the previous value of a_{13} , i.e., we perform a brute-force (quasi-adiabatic) numerical continuation. We find no recurrent clustering for values of a_{13} smaller than approximately 0.2. Beyond this value, the diagram exhibits mainly two different behaviors: ordered (periodic dynamics) and irregular (chaotic dynamics) appearance of clusters. Until $a_{13} \approx 1.0$, we observe a periodic clustering, with all cluster states present except the cluster $C_{\{1,3\},2}$ (olive green in Fig. 2). When the influence of oscillator 3 on oscillator 1 increases, i.e., for relatively large values of a_{13} , we no longer observe the periodic clustering. Instead, the structure of the diagram is highly irregular. For some large values of a_{13} , there are intervals in which the diagram becomes ordered again, resembling periodic windows in classical bifurcation diagrams [Figs. 2(a) and 2(b)]. Also, we notice the emergence of the cluster state $C_{\{1,3\},2}$. After $a_{13} \approx 1.45$, the diagram becomes regular again.

V. NUMERICAL LYAPUNOV EXPONENTS

The dynamics of the model can be quantified by calculating the Lyapunov exponents (LEs).^{51,52} In our case of only three oscillators,

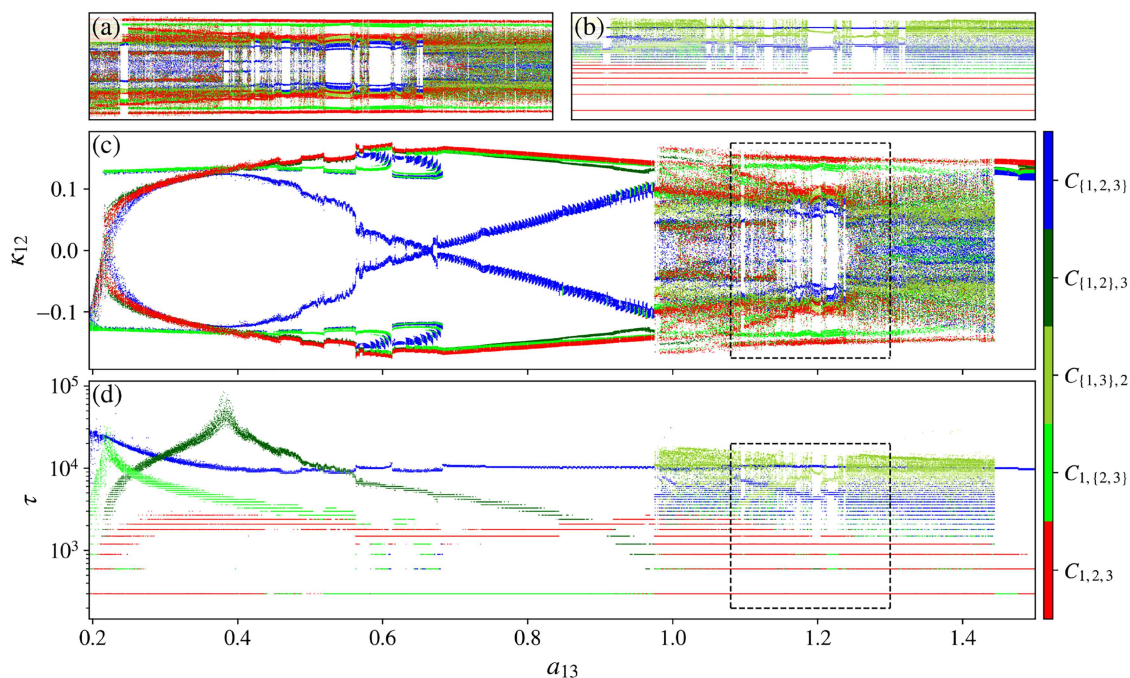


FIG. 2. (a) and (c) The value of κ_{12} when each of the clustering regimes begins, and (b) and (d) the time spent in each one of the clustering regimes as a function of a_{13} . Panels (a) and (b) are magnifications of the dashed black box in (c) and (d), respectively. The total integration time is 1.0×10^6 , the transient time is 3.0×10^5 , and the time step is 0.02. Other parameters are in Table I.

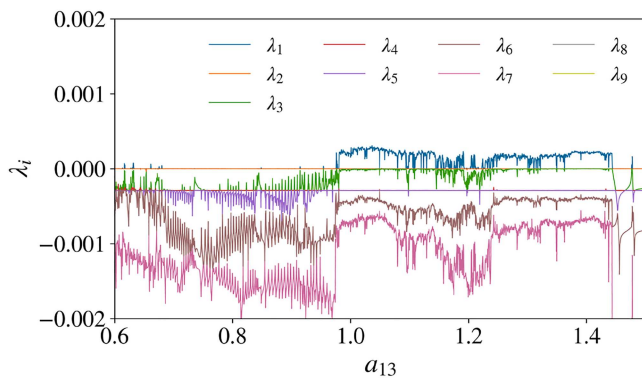


FIG. 3. The Lyapunov exponents as a function of a_{13} . The total integration time is 1.0×10^7 , the transient time is 3.0×10^5 , and the time step is 0.02. Other parameters are in Table I.

the dynamics of the fast system (the phases) for constant coupling weights (without adaptation) cannot be chaotic because the dynamics is effectively two-dimensional when written in terms of the phase differences $\theta_1 = \phi_1 - \phi_2$ and $\theta_2 = \phi_1 - \phi_3$. This is a result of the phase shift symmetry $\phi_i + \text{const}$ of the phase oscillator model. Also, additional zero LEs appear due to such a symmetry.

However, the whole adaptive model (6)–(7) is high-dimensional and can exhibit chaotic solutions. In our case, we have nine equations and hence nine characteristic exponents. Our computation of the LEs follows Benettin’s algorithm,^{51,52} which consists of integrating the linearized system simultaneously with the equations of motion and includes the Gram–Schmidt re-orthonormalization procedure. We compute the LEs as a function of the parameter a_{13} (Fig. 3) using a transient time of 3.0×10^5 and total integration time of 1.0×10^7 , with a time step of 0.02.

The periodic dynamics persists for $a_{13} \lesssim 1.0$, i.e., there are no positive LEs, and for larger a_{13} , the dynamics becomes chaotic, characterized by a positive largest Lyapunov exponent, $\lambda_1 > 0$. We observe several drops of λ_1 toward zero in the ordered regions of the bifurcation diagram (Fig. 2), indicating that these regions indeed correspond to periodic windows. Therefore, by adding a third oscillator to the network, it is possible to observe recurrent periodic synchronization as well as recurrent chaotic synchronization depending on the values of the connectivity matrix a_{ij} , which was not possible for the case of two oscillators.²⁰ Note that the small blue positive peaks of the largest Lyapunov exponent for parameter values a_{13} between 0.6 and 0.7 correspond to a state where it is difficult to distinguish numerically between weakly chaotic or quasiperiodic behavior (even using phase portraits), and we do not focus on them here.

By fixing a_{13} and changing ε (Fig. 4), we find that the largest Lyapunov exponent in the chaotic regime scales as $\sim \varepsilon$, which is an indication that the chaotic dynamics occurs on the slow timescale. Slow chaos means that the chaotic dynamics takes place on the timescale $1/\varepsilon$, and hence the largest Lyapunov exponent should be of the order of ε . This, however, does not mean that the behavior of λ_1 must be exactly linear. Exactly linear behavior would be in the case

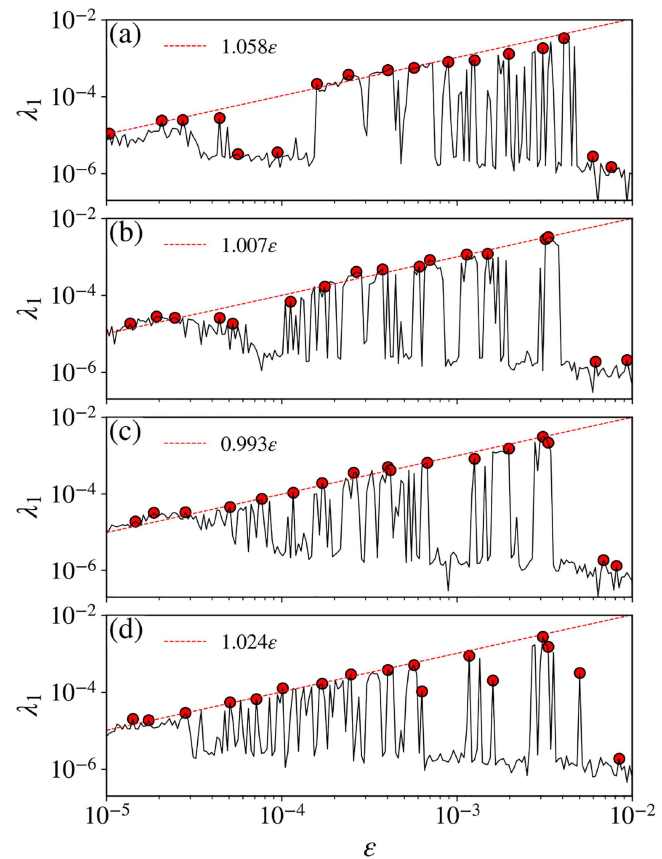


FIG. 4. The largest Lyapunov exponent, λ_1 , as a function of ε with (a) $a_{13} = 1.0$, (b) $a_{13} = 1.1$, (c) $a_{13} = 1.2$, and (d) $a_{13} = 1.3$. The red circles were obtained by performing a max pooling in windows of 12 elements and the red dashed line represents the optimal fit based on the function $f(\varepsilon) = \text{const} \times \varepsilon$ for these circles. The last two circles were excluded from this fitting process. The total integration time is 5.0×10^6 , the transient time is 3.0×10^5 , and the time step is 0.02. Other parameters are in Table I.

of a simple time rescaling of a fixed chaotic attractor. In our system here, the dynamics also changes with ε . This leads to periodic windows and λ_1 has a complex behavior. However, Fig. 4 shows that the amplitude of the oscillations of λ_1 scales proportionally to ε . Intuitively, if we look only at the maxima of λ_1 , we observe the points of “most developed” chaos between two drops of λ_1 , and this regime has a linear dependence on ε . Of course, this is not a rigorous proof of slow chaos, but rather an additional numerical support for the statement that chaos takes place on the $1/\varepsilon$ timescale. In Sec. VI, we look at the dynamics of the slow variables in more detail.

VI. DYNAMICS OF THE SLOW VARIABLES

Figure 5 displays the slow dynamics in the $(\kappa_{12}, \kappa_{21})$ plane. When the dynamics is periodic [Figs. 5(a)–5(e) and 5(g)], the projection into this plane shows limit cycles passing through regions of different synchronization regimes, which clarifies the behavior of

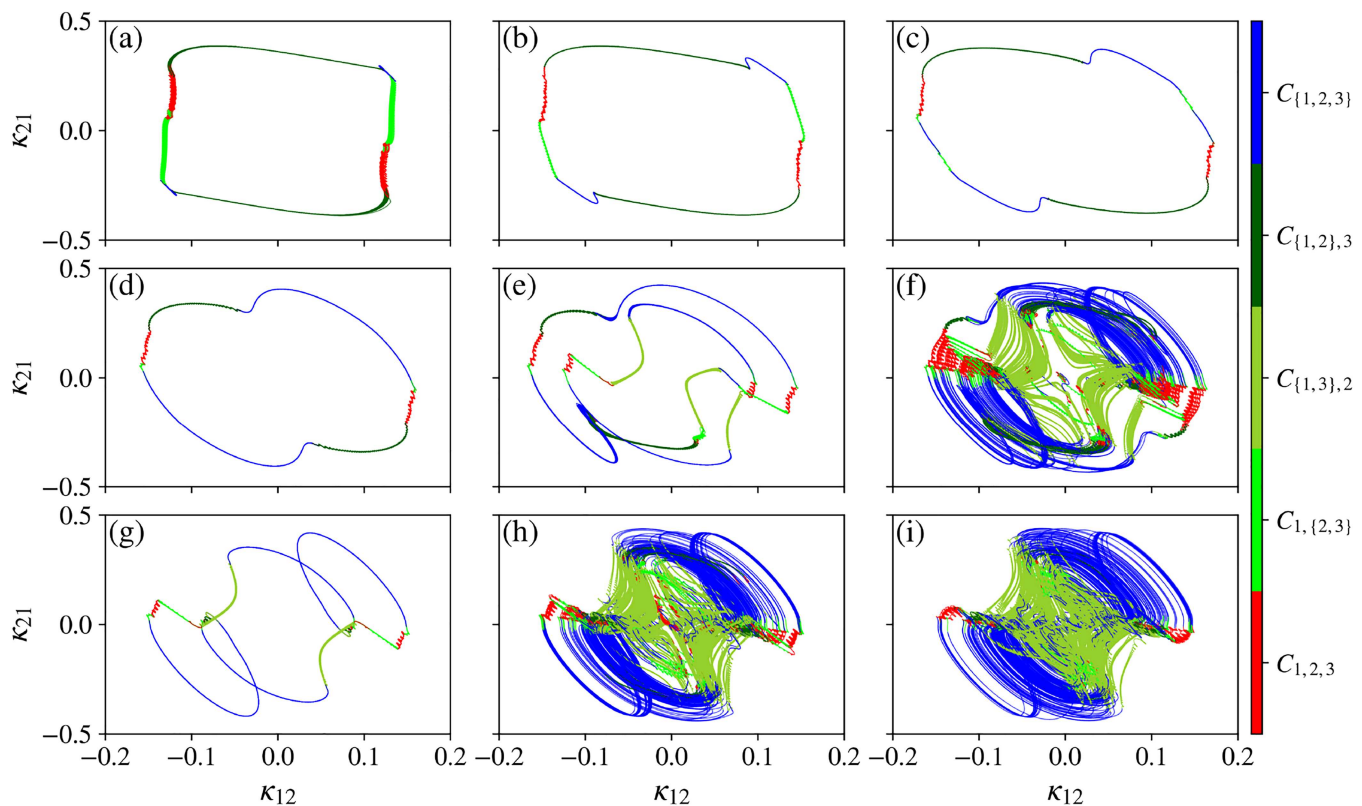


FIG. 5. Projections in the $\kappa_{12} \times \kappa_{21}$ plane for (a) $a_{13} = 0.35$, (b) $a_{13} = 0.50$, (c) $a_{13} = 0.60$, (d) $a_{13} = 0.80$, (e) $a_{13} = 1.0$, (f) $a_{13} = 1.1$, (g) $a_{13} = 1.2$, (h) $a_{13} = 1.25$, and (i) $a_{13} = 1.4$. The total integration time is 5.0×10^6 , the transient time is 3.0×10^5 , and the time step is 0.02. Other parameters are in Table I.

the order parameter in Figs. 1(b) and 1(c). The colors correspond to the type of clustering in Fig. 1. In particular, blue indicates the equilibria of the fast system (slow manifolds), and the slow motions along a set of such equilibria, when all three oscillators are frequency synchronized. The different shades of green correspond to partial clusterings (see colorbar in Fig. 5) and oscillations of the fast variables, which are averaged in the κ dynamics. This type of dynamics, which is a more complex type of recurrent synchronization than the one reported in Ref. 20, is shown in Figs. 5(f), 5(h), and 5(i). This chaotic motion is possible because the dimensionality of the slow subsystem κ_{ij} is 6, which gives enough dimensions for creating chaotic dynamics. In contrast, two adaptively coupled phase oscillators have only a two-dimensional slow subspace, which does not allow chaotic solutions. Similarly to the regular recurrent clustering motion, the chaotic clustering exhibits different partially synchronized states (green) as well as complete frequency synchronization (blue) and complete desynchronization (red), depending on the position in the κ_{ij} subspace. We emphasize that the main features for the emergence of recurrent synchronization, which we have extended to RACC, are the asymmetric adaptation rules and the temporal separation between the adaptation and the dynamics of the individual nodes, as reported by Thiele *et al.*²⁰ As for the emergence of RACC, an additional requirement is a slow subsystem with

at least three dimensions. However, a dimensionality higher than 3 alone is not enough for the emergence of RACC, as the asymmetrical adaptation rules are also essential. Therefore, a dimensionality of 3 is a necessary but not sufficient condition for the emergence of RACC.

VII. CONCLUSIONS

In summary, by using a minimal model of three adaptively coupled phase oscillators, we have presented the phenomenon of recurrent adaptive chaotic clustering (RACC). This phenomenon is characterized by quasi-stationary frequency clusters that persist for a time interval of order ε , where $1/\varepsilon$ is the slow time scale of adaptation. When a quasi-stationary cluster terminates, either a different type of cluster appears or synchrony, which is also quasi-stationary. We show that such recurrent behavior can be chaotic for a large set of parameter values. To the best of our knowledge, this phenomenon is new, and it is caused by the adaptation of the coupling weights, making it a characteristic of the class of ADNs.

From the point of view of multiscale systems,^{24,53} the presented phenomena provide an interesting example where the slow dynamics is chaotic while the fast (layer) dynamics is regular. We provide evidence for slow chaos by computing the maximal Lyapunov

exponent and its dependence on ε , as well as a brute-force bifurcation diagram and a projection of the dynamics onto a plane of two slow variables. Any theoretical proof in this direction seems to be extremely challenging, and we would wonder if such a proof appears in the future for a possibly even simpler model of an adaptive network or some other type of slow-fast system.

ACKNOWLEDGMENTS

This work was supported by the Deutsche Forschungsgemeinschaft (DFG, German Research Foundation), Project No. 411803875, the Brazilian Agencies Coordination of Superior Level Staff Improvement (CAPES) under Grant Nos. 88887.485462/2020-00 and 88881.689932/2022-01, and the São Paulo Research Foundation (FAPESP) under Grant No. 2023/08698-9.

AUTHOR DECLARATIONS

Conflict of Interest

The authors have no conflicts to disclose.

Author Contributions

Matheus Rolim Sales: Conceptualization (equal); Data curation (equal); Formal analysis (equal); Investigation (equal); Methodology (equal); Writing – original draft (equal); Writing – review & editing (equal). **Serhiy Yanchuk:** Conceptualization (equal); Data curation (equal); Formal analysis (equal); Investigation (equal); Methodology (equal); Supervision (lead); Writing – original draft (equal); Writing – review & editing (equal). **Jürgen Kurths:** Conceptualization (equal); Data curation (equal); Formal analysis (equal); Investigation (equal); Methodology (equal); Writing – original draft (equal); Writing – review & editing (equal).

DATA AVAILABILITY

The data that support the findings of this study are available within the article.

REFERENCES

- ¹L. F. Abbott and S. B. Nelson, “Synaptic plasticity: Taming the beast,” *Nat. Neurosci.* **3**, 1178–1183 (2000).
- ²W. Gerstner, W. M. Kistler, R. Naud, and L. Paninski, *Neuronal Dynamics* (Cambridge University Press, Cambridge, 2014).
- ³O. Popovych, S. Yanchuk, and P. Tass, “Self-organized noise resistance of oscillatory neural networks with spike timing-dependent plasticity,” *Sci. Rep.* **3**, 2926 (2013).
- ⁴T. Gross, C. J. D. D’Lima, and B. Blasius, “Epidemic dynamics on an adaptive network,” *Phys. Rev. Lett.* **96**, 208701 (2006).
- ⁵T. Gross and H. Sayama, “Adaptive networks,” in *Adaptive Networks: Theory, Models and Applications*, edited by T. Gross and H. Sayama (Springer Berlin Heidelberg, Berlin, 2009), pp. 1–8.
- ⁶L. Horstmeyer and C. Kuehn, “Adaptive voter model on simplicial complexes,” *Phys. Rev. E* **101**, 022305 (2020).
- ⁷F. Schweitzer, “Social percolation revisited: From 2d lattices to adaptive networks,” *Physica A* **570**, 125687 (2021).
- ⁸E. A. Martens and K. Klemm, “Cyclic structure induced by load fluctuations in adaptive transportation networks,” in *Progress in Industrial Mathematics at ECMI 2018*, edited by I. Faragó, F. Izsák, and P. L. Simon (Springer International Publishing, Cham, 2019), pp. 147–155.

- ⁹A. Pikovsky and Y. Maistrenko, *Synchronization: Theory and Application* (Kluwer Academic Publishers, 2003), Vol. 109.
- ¹⁰A. Pikovsky, M. Rosenblum, and J. Kurths, *Synchronization: A Universal Concept in Nonlinear Sciences*, Cambridge Nonlinear Science Series (Cambridge University Press, 2001).
- ¹¹R. Berner, T. Gross, C. Kuehn, J. Kurths, and S. Yanchuk, “Adaptive dynamical networks,” *Phys. Rep.* **1031**, 1–59 (2023).
- ¹²T. Gross and B. Blasius, “Adaptive coevolutionary networks: A review,” *J. R. Soc. Interface* **5**, 259–271 (2008).
- ¹³N. Caporale and Y. Dan, “Spike timing-dependent plasticity: A Hebbian learning rule,” *Annu. Rev. Neurosci.* **31**, 25–46 (2008).
- ¹⁴D. V. Kasatkin, S. Yanchuk, E. Schöll, and V. I. Nekorkin, “Self-organized emergence of multilayer structure and chimera states in dynamical networks with adaptive couplings,” *Phys. Rev. E* **96**, 62211 (2017).
- ¹⁵R. Berner, E. Schöll, and S. Yanchuk, “Multiclusters in networks of adaptively coupled phase oscillators,” *SIAM J. Appl. Dyn. Syst.* **18**, 2227–2266 (2019).
- ¹⁶P. Feketa, A. Schaum, and T. Meurer, “Synchronization and multicluster capabilities of oscillatory networks with adaptive coupling,” *IEEE Trans. Automat. Control* **66**, 3084–3096 (2021).
- ¹⁷O. V. Popovych, M. N. Xenakis, and P. A. Tass, “The spacing principle for unlearning abnormal neuronal synchrony,” *PLoS One* **10**, e0117205 (2015).
- ¹⁸T. Aoki, “Self-organization of a recurrent network under ongoing synaptic plasticity,” *Neural Netw.* **62**, 11–19 (2015).
- ¹⁹V. Röhr, R. Berner, E. L. Lameu, O. V. Popovych, and S. Yanchuk, “Frequency cluster formation and slow oscillations in neural populations with plasticity,” *PLoS One* **14**, e0225094 (2019).
- ²⁰M. Thiele, R. Berner, P. A. Tass, E. Schöll, and S. Yanchuk, “Asymmetric adaptivity induces recurrent synchronization in complex networks,” *Chaos* **33**, 023123 (2023).
- ²¹S. Bornholdt and T. Röhl, “Self-organized critical neural networks,” *Phys. Rev. E* **67**, 066118 (2003).
- ²²J. Fialkowski, S. Yanchuk, I. M. Sokolov, E. Schöll, G. A. Gottwald, and R. Berner, “Heterogeneous nucleation in finite-size adaptive dynamical networks,” *Phys. Rev. Lett.* **130**, 067402 (2023).
- ²³C. Kuehn, “Multiscale dynamics of an adaptive catalytic network,” *Math. Model. Nat. Phenom.* **14**, 402 (2019).
- ²⁴C. Kuehn, *Multiple Time Scale Dynamics* (Springer-Verlag GmbH, 2015), Vol. 191.
- ²⁵S. H. Strogatz, “Exploring complex networks,” *Nature* **410**, 268–276 (2001).
- ²⁶S. Boccaletti, V. Latora, Y. Moreno, M. Chavez, and D.-U. Hwang, “Complex networks: Structure and dynamics,” *Phys. Rep.* **424**, 175–308 (2006).
- ²⁷A. S. d. Mata, “Complex networks: A mini-review,” *Braz. J. Phys.* **50**, 658–672 (2020).
- ²⁸Y. Zou, R. V. Donner, N. Marwan, J. F. Donges, and J. Kurths, “Complex network approaches to nonlinear time series analysis,” *Phys. Rep.* **787**, 1–97 (2019).
- ²⁹O. V. Maslennikov and V. I. Nekorkin, “Adaptive dynamical networks,” *Phys. Usp.* **60**, 694 (2017).
- ³⁰J. Sawicki, R. Berner, S. A. M. Loos, M. Anvari, R. Bader, W. Barfuss, N. Botta, N. Brede, I. Franovi, D. J. Gauthier, S. Goldt, A. Hajizadeh, P. Hövel, O. Karin, P. Lorenz-Spreen, C. Miehl, J. Mölter, S. Olmi, E. Schöll, A. Seif, P. A. Tass, G. Volpe, S. Yanchuk, and J. Kurths, “Perspectives on adaptive dynamical systems,” *Chaos* **33**, 071501 (2023).
- ³¹C. Zhou and J. Kurths, “Dynamical weights and enhanced synchronization in adaptive complex networks,” *Phys. Rev. Lett.* **96**, 164102 (2006).
- ³²M. Wiedermann, J. F. Donges, J. Heitzig, W. Lucht, and J. Kurths, “Macroscopic description of complex adaptive networks coevolving with dynamic node states,” *Phys. Rev. E* **91**, 052801 (2015).
- ³³E. A. Martens and K. Klemm, “Transitions from trees to cycles in adaptive flow networks,” *Front. Phys.* **5**, 62 (2017).
- ³⁴B. Duchet, C. Bick, and A. Byrne, “Mean-field approximations with adaptive coupling for networks with spike-timing-Dependent plasticity,” *Neural Comput.* **35**, 1481–1528 (2023).
- ³⁵T. Aoki and T. Aoyagi, “Co-evolution of phases and connection strengths in a network of phase oscillators,” *Phys. Rev. Lett.* **102**, 034101 (2009).

- ³⁶R. Berner, S. Vock, E. Schöll, and S. Yanchuk, “Desynchronization transitions in adaptive networks,” *Phys. Rev. Lett.* **126**, 028301 (2021).
- ³⁷B. Jüttner and E. A. Martens, “Complex dynamics in adaptive phase oscillator networks,” *Chaos* **33**, 053106 (2023).
- ³⁸H. Markram, W. Gerstner, and P. J. Sjöström, “Spike-timing-dependent plasticity: A comprehensive overview,” *Front. Synaptic Neurosci.* **4**, 2 (2012).
- ³⁹N. Fenichel, “Geometric singular perturbation theory for ordinary differential equations,” *J. Differ. Equ.* **31**, 53–98 (1979).
- ⁴⁰M. Krupa and P. Szmolyan, “Relaxation oscillation and canard explosion,” *J. Differ. Equ.* **174**, 312–368 (2001).
- ⁴¹P. Szmolyan and M. Wechselberger, “Canards in R^3 ,” *J. Differ. Equ.* **177**, 419–453 (2001).
- ⁴²S. Wicczorek, P. Ashwin, C. M. Luke, and P. M. Cox, “Excitability in ramped systems: The compost-bomb instability,” *Proc. R. Soc. A* **467**, 1243–1269 (2011).
- ⁴³M. Ciszak, F. Marino, A. Torcini, and S. Olmi, “Emergent excitability in populations of nonexcitable units,” *Phys. Rev. E* **102**, 050201 (2020).
- ⁴⁴Y. Kuramoto, *Chemical Oscillations, Waves, and Turbulence*, Springer Series in Synergetics Vol. 19 (Springer Berlin Heidelberg, Berlin, 1984).
- ⁴⁵H. Sakaguchi and Y. Kuramoto, “A soluble active rotator model showing phase transitions via mutual entertainment,” *Prog. Theor. Phys.* **76**, 576–581 (1986).
- ⁴⁶F. C. Hoppensteadt and E. M. Izhikevich, *Neuron*, Applied Mathematical Sciences Vol. 126 (Springer New York, New York, 1997).
- ⁴⁷B. Pietras and A. Daffertshofer, “Network dynamics of coupled oscillators and phase reduction techniques,” *Phys. Rep.* **819**, 1–105 (2019).
- ⁴⁸A. L. Hodgkin and A. F. Huxley, “A quantitative description of membrane current and its application to conduction and excitation in nerve,” *J. Phys.* **117**, 500–544 (1952).
- ⁴⁹A. Bergner, M. Frasca, G. Sciuto, A. Buscarino, E. J. Ngamga, L. Fortuna, and J. Kurths, “Remote synchronization in star networks,” *Phys. Rev. E* **85**, 026208 (2012).
- ⁵⁰I. Leyva, I. Sendiña-Nadal, R. Sevilla-Escoboza, V. P. Vera-Avila, P. Chholak, and S. Boccaletti, “Relay synchronization in multiplex networks,” *Sci. Rep.* **8**, 8629 (2018).
- ⁵¹G. Benettin, L. Galgani, A. Giorgilli, and J.-M. Strelcyn, “Lyapunov characteristic exponents for smooth dynamical systems and for Hamiltonian systems; a method for computing all of them. Part 1: Theory,” *Meccanica* **15**, 9–20 (1980).
- ⁵²A. Wolf, J. B. Swift, H. L. Swinney, and J. A. Vastano, “Determining Lyapunov exponents from a time series,” *Physica D* **16**, 285–317 (1985).
- ⁵³A. Vanselow, S. Wicczorek, and U. Feudel, “When very slow is too fast—Collapse of a predator-prey system,” *J. Theor. Biol.* **479**, 64–72 (2019).